

Dual Solution of Unsteady Boundary Layer Flow of Viscose Fluid Over a Stretching Cylinder Considering Thermal Conductivity Effects

Shefali Jauhari¹, Upendra Mishra²

¹Department of Mathematics, Invertis University, Rajau Paraspur, National Highway NH 30, Bareilly, Uttar Pradesh 243123, Shefali.j@invertis.org

²Department of Mathematics, Amity University Rajasthan, NH-11 C, Kant Kalwar, Delhi-Jaipur Highway, Near Achrol Village, Jaipur, INDIA

Abstract

The study has analyzed the magnetohydrodynamics (MHD) unsteady boundary layer flow of a viscous fluid over a stretching cylinder, considering thermal conductivity effects. The graphical analysis delves into the influence of various flow parameters on the profiles of flow velocity and temperature. By employing similarity transformations, the governing equations transform. Subsequently, these transformed equations are numerically solved using the shooting method. The investigation uncovers the presence of dual solutions with increasing parameters such as velocity slip, magnetic field strength, and suction effect. Various physical parameters are meticulously examined and discussed. Furthermore, numerical analyses are performed to ascertain expressions for the skin friction coefficient, Nusselt number, fluid velocity, and temperature around the cylinder, with their variations elucidated through graphical representations.

Keywords: Unsteady Boundary layer flow, Dual solutions, Momentum slip condition, Thermal slip condition.

1. INTRODUCTION:

As technological advancements continue to progress, the study of steady viscous flow with mass transfer over a stretching cylinder has garnered significant attention from scientists and engineers. This is primarily due to its wide-ranging industrial applications, including metal mining, extrusion, wire drawing, and the processing of copper wire. The flow dynamics and heat transfer characteristics occurring within the boundary layer of elongating flat plates or cylinders play a crucial role in fiber technology and extrusion processes. These processes are vital across various industrial manufacturing sectors, involving the production of sheeting materials made of metals or polymers. The uses vary widely, including cooling metallic plates in a bath, controlling boundary layers on material conveyors, aerodynamically shaping plastic sheets, dealing with liquid films in condensation processes, producing paper, blowing glass, spinning metal, drawing plastic films, and extruding polymers. The overall quality of the end product is significantly influenced by how effectively heat is transferred at the stretching surface. Cylindrical slip flow has various applications in microfluidics, nanotechnology, and engineering at small scales. Understanding slip flow is essential for the design and optimization of microfluidic devices, where the effects of slip can significantly influence the performance and behaviour of fluids in confined geometries. Researchers and engineers often use specialized models and computational simulations to analyze and predict slip flow behavior accurately.

In a groundbreaking study, in recent investigations, multiple researchers [1–4] have examined flow issues involving the inclusion of partial slip effects at the extending wall and the presence of a magnetic field introduces a novel aspect to the research. Adigun et al. [5] explore the magnetohydrodynamic (MHD) stagnation point flow of a viscoelastic nanofluid around an inclined cylinder undergoing linear stretching. The presence of dual solutions in unsteady boundary layer flow over a cylindrical sheet has been explored in several studies. Bhattacharyya [6] discovered the presence of dual solutions for specific parameters. Crane [7] explored the analysis of the flow arising from the stretching of a sheet. Datta et al. [8] proposed potential applications involving emergency shutdowns in nuclear reactors through cooling, where specific areas could be cooled by introducing a coolant. and Dey [9] discovered the presence of dual solutions for specific parameters, delving deeper into the stability analysis of these solutions. Ellahi et al. [10] explored the analysis of steady viscous liquid flow, incorporating a nonlinear slip condition, utilizing both analytic solutions and numerical solutions for flow analysis. Fadzilah [11] asserts that the numerical solutions maintain consistent validity across all dimensionless time intervals, encompassing the transition from the initial unsteady-state flow to the eventual steady-state flow, across the entirety of the spatial domain.

Hayat et al. [12-13] investigated the colloidal properties of ferrofluid when subjected to a magnetic dipole and Flow at the stagnation point with non-Fourier heat flux and reactions involving both homogeneous and heterogeneous processes were also examined. The impact of magnets on horizontally and vertically elongated

cylinders was explored by Ishak et al. [14]. Ishak and Nazar [15] proposed the possibility of achieving similar solutions by considering the stretching cylinder with a linear velocity. Jagan [16] investigated Research into convective flow, which involves the transfer of heat and mass and has garnered significant attention due to its broad applications in numerous fields. This study delves into how nonlinear thermal radiation slip, thermal diffusion, and diffusion-thermo effects influence magnetohydrodynamic flow toward a stretching cylinder, with a focus on triple stratification (TSF). Jauhri S and Mishra U [17-19] studied the dual solution under second-order slip boundary conditions. Lin and Shih [20-21] concentrated on examining the smooth boundary layer and heat transfer surrounding cylinders moving steadily, either horizontally or vertically. Mahapatra and Gupta [22] examined the viscous fluid in a two-dimensional, considering the flow over an extended surface with heat transfer at a stagnation point. Mahapatra [23] expanded upon this research by incorporating the influences of viscoelasticity and magnetic fields, identifying the persistence of dual solutions under specific conditions. They acknowledged the challenges in obtaining comparable results due to the influence of the cylinder's curvature.

Mishra. et al [24] examined an analytical solution of the MHD flow of two visco-elastic fluids over a sheet shrinking with quadratic velocity. Mukhopadhyay [25-26] conducted a study on the impact of a uniform magnetic field on the axisymmetric laminar boundary layer flow of a viscous, incompressible fluid towards a stretching cylinder, taking into account heat transfer effects. Nazar [27] also contributed to this area of research by studying the transition from the initial unsteady state flow to the final steady-state flow. Several researchers [28-31] investigations have delved into the dynamics of magnetohydrodynamics (MHD) in unsteady boundary layer flow over a stretching cylinder, examining a range of influential factors. Furthermore, as research in this area progresses, it is crucial to critically evaluate the significance of slip flow and magnetohydrodynamics in practical engineering and scientific contexts.

This study aims to investigate the influence of thermal conductivity on the MHD unsteady boundary layer flow of a viscous fluid over a stretching cylinder and to provide a better understanding of the fluid flow and heat transfer phenomena in industrial and engineering applications. Future studies should aim to address the potential discrepancies on theoretical predictions, providing a more comprehensive understanding of the implications of slip flow and magnetic field effects in fluid dynamics. The impact of slip conditions, magnetic parameters, and other physical and geometric parameters on fluid and temperature profiles has been thoroughly analyzed. The influence of magnetic fields on fluid flow, specifically the alteration of flow patterns in regions dominated by Lorentz forces, has been elucidated, emphasizing the fundamental aspect of magnetohydrodynamics

2. Mathematical Formulation: We examined the characteristics of a time-dependent viscous, incompressible fluid flowing steadily in an axisymmetric manner along a cylinder undergoing elongation, all under the influence of a uniform magnetic field, as illustrated in Figure 1. Furthermore, it is assumed that the cylinder's diameter varies over time, with the radius undergoing unsteady changes $a(t) = a_0\sqrt{1 - \beta t}$, where a_0 is a constant and β is a constant of expansion/contraction. In this depiction, the x-axis represents the cylinder's axis, and the r-axis extends radially. We assume a uniform magnetic field with an intensity B_0 acting radially. To simplify matters, we assume that the magnetic Reynolds number is small, meaning that the induced magnetic field can be disregarded compared to the applied magnetic field. Additionally, we posit that the temperature at the surface of the cylinder varies over time as a function of both position along the z-axis and time, denoted as $T_w(z, t)$, with T_w being greater than the ambient fluid temperature. The governing equations for continuity, momentum, and energy in this specific flow setup can be expressed as follows:

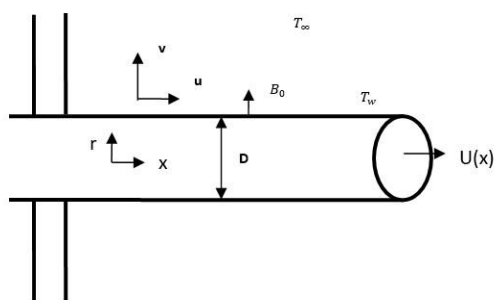


Fig.1. Illustration of the physical Model.

$$\frac{\partial(ru)}{\partial x} + \frac{\partial(rv)}{\partial r} = 0 \quad (2.1)$$

$$\frac{\partial u}{\partial t} + u \frac{\partial u}{\partial x} + v \frac{\partial u}{\partial r} = \frac{\nu}{r} \frac{\partial}{\partial r} \left(r \frac{\partial u}{\partial r} \right) - \frac{\sigma B_0^2}{\rho} (U) - g\beta_T (T - T_\infty) \quad (2.2)$$

$$\frac{\partial T}{\partial t} + u \frac{\partial T}{\partial x} + v \frac{\partial T}{\partial r} = \frac{\kappa}{\rho c_p} \frac{\partial}{\partial r} \left(r \frac{\partial T}{\partial r} \right) \quad (2.3)$$

Where u and v are the velocity components correspondingly aligned with the x -direction and r -direction, $\nu = \frac{\mu}{\rho}$ is the kinematic-viscosity, fluid density (ρ), dynamics fluid viscosity coefficient (μ), electrical conductivity (σ), uniform magnetic field (B_0), thermal-diffusivity (κ) of the fluid, fluid temperature (T).

Boundary Conditions

$$u = \varepsilon \frac{1}{a_0^2} \frac{4vx}{1-\beta t} + S_1 v \frac{\partial u}{\partial r} + S_2 v \frac{\partial^2 u}{\partial r^2} \left. \vphantom{\frac{1}{a_0^2} \frac{4vx}{1-\beta t}} \right\} \text{at } r = D \quad (2.4)$$

$$T = T_w + \frac{bx}{a_0 v(1-\beta t)}$$

$$\left. \begin{array}{l} u \rightarrow 0 \\ T \rightarrow T_\infty \end{array} \right\} \text{at } r \rightarrow \infty \quad (2.5)$$

In reference of velocity, S_1 and S_2 are slip parameters and kinematic-viscosity is ' ν '. Here q_1 temperature slip parameters in reference of temperature and concentration. $U = \frac{cx}{\sqrt{1-\beta t}}$, is the stretching velocity for $\varepsilon = 1$ and shrinking velocity for $\varepsilon = -1$.

2.1 Coefficient of Skin friction

The parameters under investigation are the skin friction coefficient $C_f = \frac{\tau_w}{\rho U^2}$ at the cylinder's surface is defined as $\frac{1}{2} \sqrt{Re} C_f = h''(0)$.

2.2 Coefficient of Nusselt number

The local Nusselt number Nu , is characterized as the heat transfer rate, at the cylinder's surface is defined as $\frac{Nu}{\sqrt{Re}} = -t'(0)$.

3 Method of Solution:

The continuity equation is fulfilled by incorporating the stream function ψ as $u = \frac{1}{r} \frac{\partial \psi}{\partial r}$ and $v = -\frac{1}{r} \frac{\partial \psi}{\partial x}$.

Introducing the similarity variables as,

$$\xi = \left(\frac{r}{a_0} \right)^2 \frac{1}{1-\alpha t}, u = \frac{1}{a^2} \frac{4vx}{1-\alpha t} h'(\xi), v = \frac{-1}{a^2} \frac{2v}{1-\alpha t} \frac{h(\xi)}{\sqrt{\xi}}, \theta(\xi) = \frac{T-T_\infty}{T_w-T_\infty} \quad (3.1)$$

$$\xi h''' + h'' - h'^2 + hh'' - Meh' - S'(f' + \xi f'') + Gr\theta = 0 \quad (3.2)$$

$$\xi t'' + t' + Pr(ht' - h't - S'(\xi t' + t)) = 0 \quad (3.3)$$

Boundary Condition

$$\left. \begin{array}{l} h(\xi) = S, h'(\xi) = a + \beta_1 h''(\xi) + \beta_2 h'''(\xi) \\ t(\xi) = 1 + \delta_1 t'(\xi) \end{array} \right\} \text{at } \xi = 0 \quad (3.4)$$

$$\left. \begin{array}{l} h'(\xi) \rightarrow 0 \\ t(\xi) \rightarrow 0 \end{array} \right\} \text{at } \xi \rightarrow \infty. \quad (3.5)$$

Where $\beta_1 = S_1 \sqrt{\frac{\nu U_0}{a_0(1-\beta t)L}}$ and $\beta_2 = S_2 \frac{U_0}{a_0(1-\beta t)L}$, $a = 1/(-1)$ for stretching/ shrinking cylinder, $a = 0$ for

static-cylinder and are referred to as the 2nd and 3rd order coefficients of slip parameters. $\delta_1 = q_1 \sqrt{\frac{bU_0}{va_0(1-\beta t)L}}$

are referred to as the slip coefficient of heat transfer.

Result and Discussion: Equations (3.2) and (3.3) and their associated boundary conditions (3.4) have been solved using numerical methods. The analysis reveals the existence of two separate solutions within the system. To assess the accuracy of the numerical method used, we compared our current results for the heat transfer coefficient ($-t'(0)$) under some condition. These comparisons are summarized in Table 1, showing close agreement with previous studies. Additionally, Table 2 presents numerical data for the stretching cylinder incorporating 2nd -order slip boundary conditions. Figures 2(a, b) depict a decline in both (first and second) fluid velocity as s increases. In Fig. 3(a), it's evident that the fluid velocity rises as β_2 increases, suggesting a positive correlation between these variables. Conversely, Fig. 3(b) indicates a decrease in fluid velocity with increasing β_2 . This contrasting trend might arise from varying conditions or factors affecting the system. Figures 4(a, b) depict a decline in both (first and second) temperature with increasing β_2 . Additionally, a decrease in the thickness of the velocity boundary layer is noted with increasing s , aligning with the concept that boundary layer thickness diminishes with heightened suction.

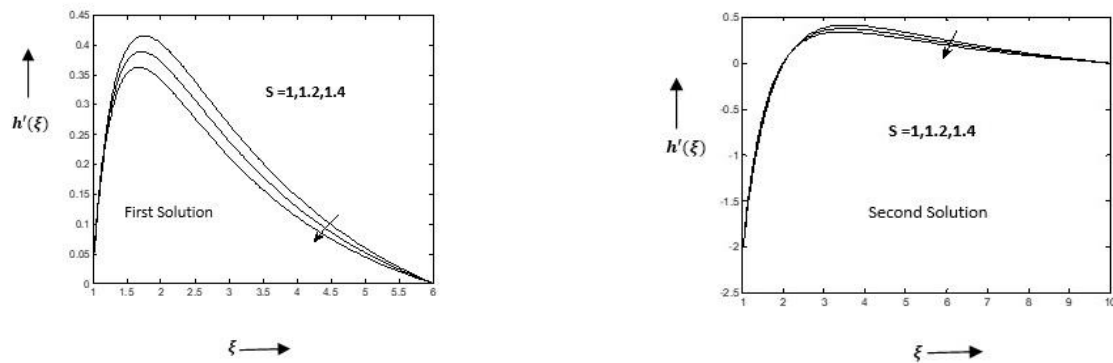


Fig. 2(a & b): Fig.2(a) and 2(b) variation of h' vs ξ across various values ' s ' when $\beta_1 = 0.1, \beta_2 = 0.1, \delta_1 = 0.1, K = 0.1, M_e = 0.1$ for the 1st and 2nd solution.

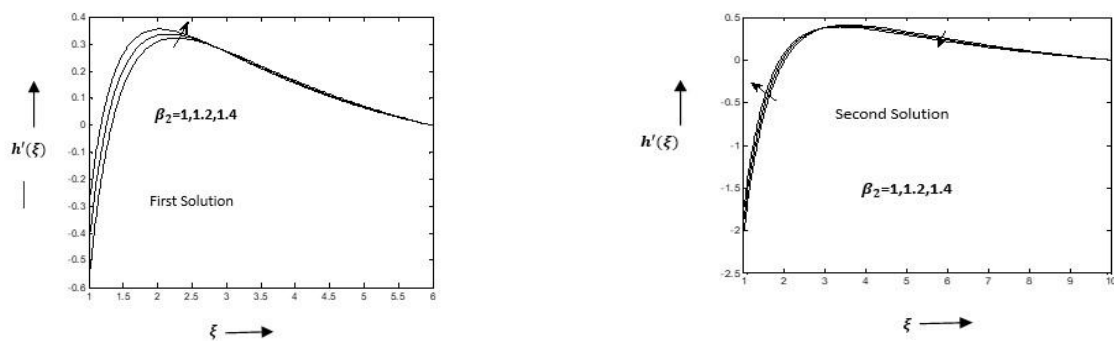


Fig. 3(a & b): Fig.3(a) and 3(b) variation of h' vs ξ across various values ' β_2 ' when $\beta_1 = 0.1, s = 0.1, \delta_1 = 0.1, K = 0.1, M_e = 0.1$ for the 1st and 2nd solution.

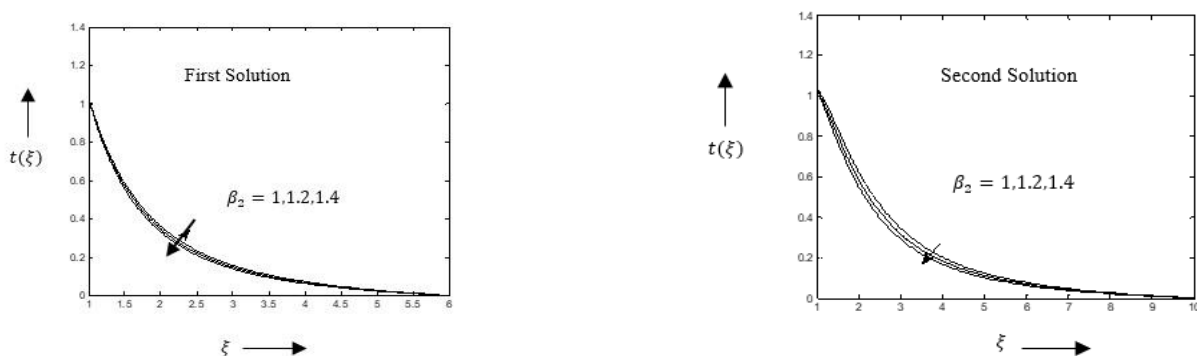


Fig. 4(a & b): Fig.4(a) and 4(b) variation of t vs ξ across various values ' β_2 ' when $\beta_1 = 0.1, s = 0.1, \delta_1 = 0.1, K = 0.1, M_e = 0.1$ for the 1st and 2nd solution.

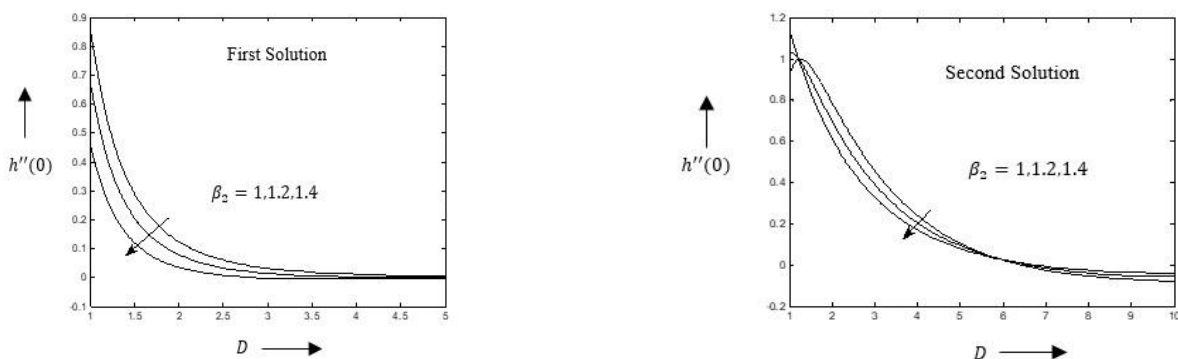


Fig. 5(a & b): Fig.5(a) and 5(b) variation of $h''(0)$ vs D across various values ' β_2 ' when $\beta_1 = 0.1, s = 0.1, \delta_1 = 0.1, K = 0.1, M_e = 0.1$ for the 1st and 2nd solution.

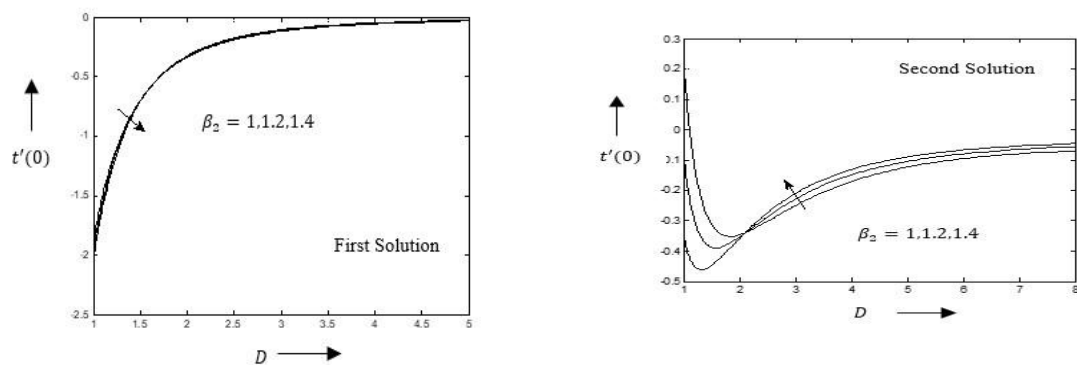


Fig. 6(a & b): Fig.6(a) and 6(b) variation of $t'(0)$ vs D across various values ' β_2 ' when $\beta_1 = 0.1, s = 0.1, \delta_1 = 0.1, K = 0.1, M_e = 0.1$ for the 1st and 2nd solution.

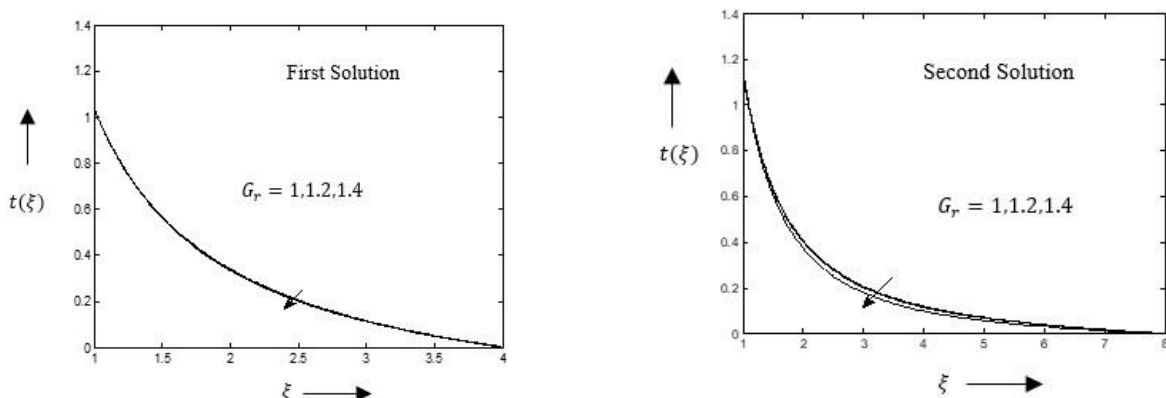


Fig. 7(a & b): Fig.7(a) and 7(b) variation of t vs ξ across various values ' G_r ' when $\beta_1 = 0.1, s = 0.1, \delta_1 = 0.1, \beta_2 = 0.1, K = 0.1, M_e = 0.1$ for the 1st and 2nd solution.

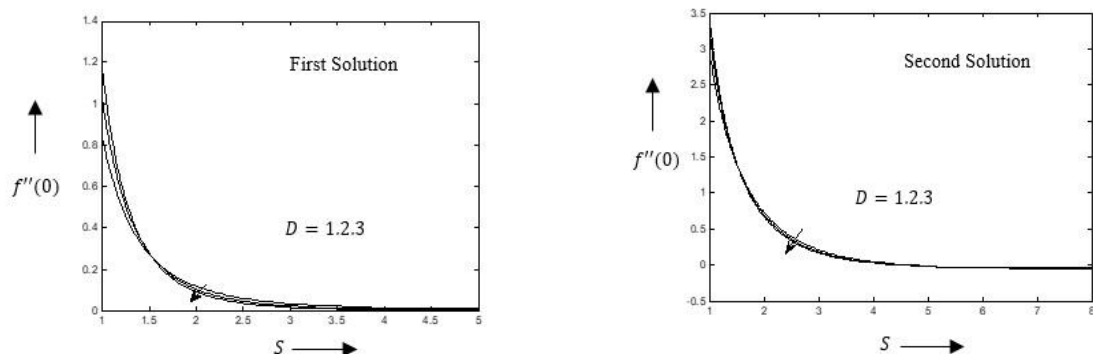


Fig. 8(a & b): Fig.8(a) and 8(b) variation of $f''(0)$ vs S across various values ' D ' when $\beta_1 = 0.1, s = 0.1, \delta_1 = 0.1, \beta_2 = 0.1, K = 0.1, M_e = 0.1$ for the 1st and 2nd solution.

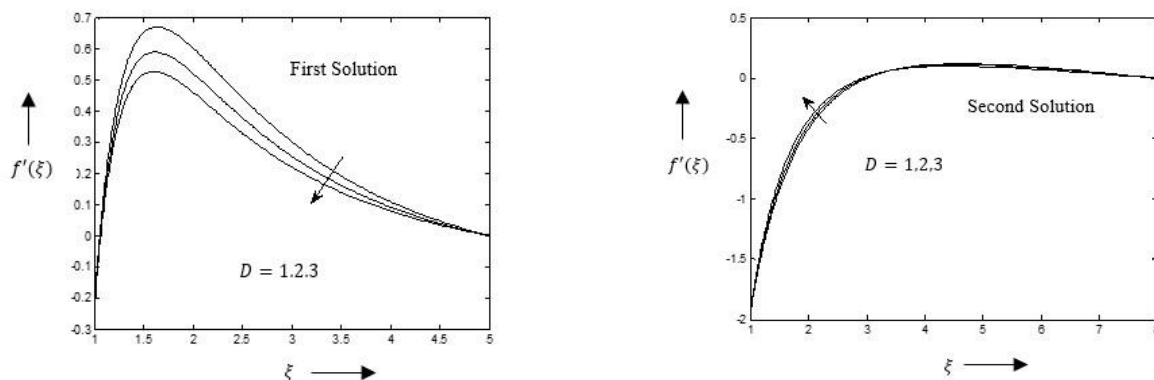


Fig. 9(a & b): Fig.9(a) and 9(b) variation of $f'(\xi)$ vs ξ across various values ' D ' when $\beta_1 = 0.1, s = 0.1, \delta_1 = 0.1, \beta_2 = 0.1, K = 0.1, M_e = 0.1$ for the 1st and 2nd solution.

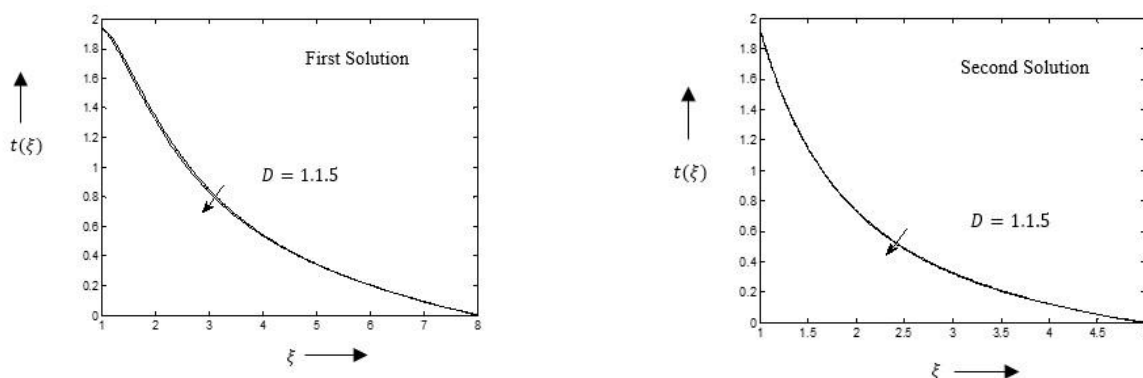


Fig. 10(a & b): Fig.10(a) and 10(b) variation of $t'(\xi)$ vs ξ across various values 'D' when $\beta_1 = 0.1, s = 0.1, \delta_1 = 0.1, \beta_2 = 0.1, K = 0.1, M_e = 0.1$ for the 1st and 2nd solution.

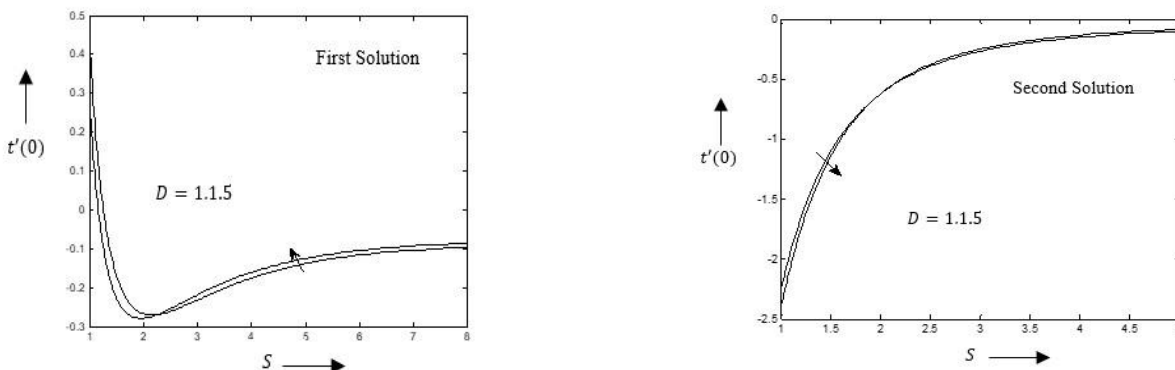


Fig. 11(a & b): Fig.11(a) and 11(b) variation of $t'(0)$ vs s across various values 'D' when $\beta_1 = 0.1, s = 0.1, \delta_1 = 0.1, \beta_2 = 0.1, K = 0.1, M_e = 0.1$ for the 1st and 2nd solution.

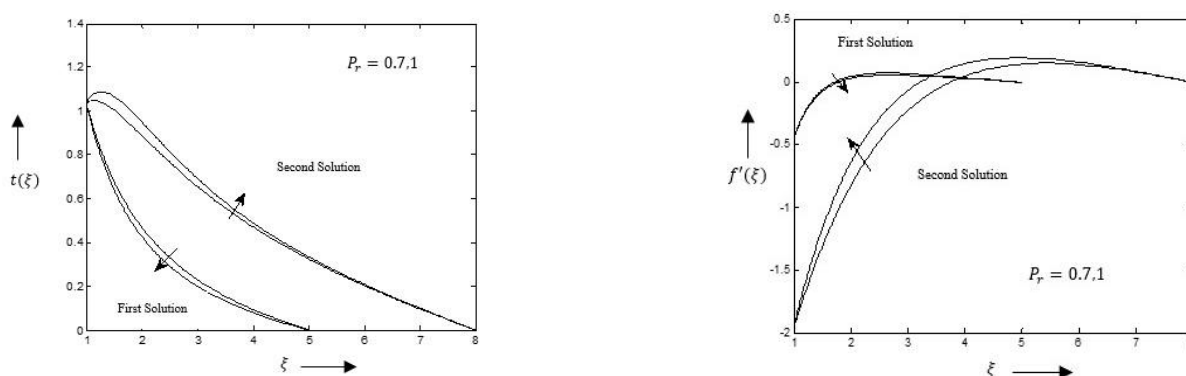


Fig. 12: Fig.12 variation of $t(\xi)$ vs ξ across various values ' P_r ' when $\beta_1 = 0.1, s = 0.1, \delta_1 = 0.1, \beta_2 = 0.1, K = 0.1, M_e = 0.1$ for the 1st and 2nd solution and **Fig. 13** variation of $f'(\xi)$ vs ξ across various values ' P_r ' when $\beta_1 = 0.1, s = 0.1, \delta_1 = 0.1, \beta_2 = 0.1, K = 0.1, M_e = 0.1$ for the 1st and 2nd solution.

Table1:- The values of $h''(1)$ & $h''(-1)$ are determined for various conditions of zero magnetic field ($Me = 0$) and Prandtl number $P_r = 0.7$.

S'	S	Zaimi et al [32]		Z. Abbas et al. [33]		Present Study	
-4.0	0.1	3.8407	-24.8822	3.8407	-24.8822	3.84068	-24.88231
-3.5		3.2990	-17.4731	3.2990	-17.4731	3.2991	-17.4731
-3.0		2.7397	-11.4552	2.73978	-11.4552	2.73978	-11.45511
-4.0	1.0	4.7879	-34.6868	4.7879	-34.6868	4.7879	-34.6868
-3.5		4.2610	-25.3598	4.2610	-25.3598	4.2610	-25.3598
-3.0		3.7255	-17.5911	3.7255	-17.5911	3.7255	-17.5911

Table 2:-Values of $[h''(1)]$ and $[-t'(1)]$ for several values of different parameter and magnetic parameter $Me = 0.1$.

S	β_1	G_r	P_r	D	$h''(1)$	$-t'(1)$
-3.5	0.2	0.1	0.7	0.1	-3.9491	-3.0923
-3.0					-3.5067	-2.7554
-2.0					-2.6436	-2.1092
-3.0	0				3.2701	-2.2703
	0.5				3.7125	-2.2234
-3.0	1.5				4.5385	-2.1246
	0.5		1		3.6957	-3.2433
			5		3.6652	17.517
			7		3.6632	-24.7422

Figure 5(a, b) shows that as β_2 increases $h''(0)$ decreases in both the solution, as β_2 increases. Moving on to Fig. 6(a & b), both subfigures illustrate a decline in fluid temperature as β_2 increases. This inverse relationship implies that as β_2 , increases, the fluid temperature tends to decrease. These observations provide valuable insights into the dynamics of the system under study, highlighting the interplay between fluid velocity, temperature, and the parameter β_2 . In Figure 6(a, b), the influence of β_2 on $-t'(0)$ is observed to decrease in the 1st solution; however, for the 2nd solution, it increases. Figures 7(a, b) depict a decline in both (first and second) fluid temperature as G_r increases. As the parameter D increases, a noticeable trend emerges where the $h''(0)$ experiences a decrease, as illustrated in Figures 8(a b). This behavior persists up to specific heights, after which the deceleration process becomes more gradual. The magnetic parameter D plays a significant role in shaping the results, suggesting that the existence of a magnetic field imposes more restrictions on the fluid, leading to a decrease in fluid velocity.

Observations from Fig. 9(a, b) for the 1st solution indicate that as the magnetic parameter D increases, h' increases, while decreases in 2nd solution. Concerning the 2nd solution, it's noted that the domain of existence for the 2nd solution expands. Figures 10(a & b) depict temperature profiles $t(\xi)$ for different D values. Across all cases, the velocity reaches zero at a noticeable distance. In both the solution, temperature decreases as the magnetic parameter D increases. Figures 11(a & b) depict temperature profiles $t'(0)$ for different D values. In the first solution, it increases as the magnetic parameter D increases while in second it decreases. Figure 12 demonstrates that as the Prandtl number increases, fluid temperature decreases in first while increases in second. i.e the thermal boundary layer thickness decreases with an increase in the Prandtl number. Figure 13 demonstrates that as the Prandtl number increases, fluid velocity decreases in first while increases in second.

CONCLUSION:-

A numerical study was conducted on the unsteady boundary layer flow around a stretching cylinder, revealing two distinct solutions: the first (1st) and second (2nd) solutions. It's noteworthy that the domain where the 2nd solution applies varies with changes in physical parameters. In the 1st solution, variations in suction result in the convergence of profiles of $h'(\xi)$ and $t(\xi)$, leading to reduced velocity and thermal boundary layer thicknesses. Specifically, the velocity boundary layer thickness decreases with increasing suction parameter in the 1st solution, indicating its practical importance. However, the 2nd solution mainly arises as a mathematical artifact from the model and doesn't exhibit consistent trends with changes in physical parameters. Slip conditions near the boundary where slip occurs cause a decrease in the stream function, signifying a reduction in volume flux or flow rate in that specific region. Increasing the magnetic parameter can reduce the stream function in regions dominated by Lorentz forces, thereby altering the flow pattern. This highlights the magnetic field's influence on fluid flow, a fundamental aspect of magnetohydrodynamics. Nonetheless, except for the slip parameter (1st-order), the temperature profiles of both solutions show similar trends as physical parameters vary. Additionally, geometric parameters like the curvature parameter and Prandtl number affect fluid and temperature profiles. At higher Prandtl numbers, both velocity and temperature boundary layers tend to thicken due to increased diffusive effects.

REFERENCES:-

1. Andersson H.I., (2002): Slip flow past a stretching surface. Acta Mech; vol.158, pp.121–126.

2. Ariel P.D., Hayat T, Asghar S, (2006): The flow of an elasticoviscous fluid past a stretching sheet with partial slip. *Acta Mech*, vol.187, pp.29–35.
3. Ariel P.D., (2008): Two-dimensional stagnation point flow of an elasticoviscous fluid with partial slip. *ZAMM Journal of Applied Mathematics and mechanics*, vol.88, pp.320–324.
4. Abbas Z, Wang Y, Hayat T, Oberlack M. (2009): Slip effects and heat transfer analysis in a viscous fluid over an oscillatory stretching surface. *Int J Numer Meth Fluids*, vol. 59, pp.443–58.
5. Adigun J.A, Adeniyi A, Abiala I.O,(2021): Stagnation point MHD slip-flow of viscoelastic nanomaterial over a stretched inclined cylindrical surface in a porous medium with dual stratification. *International Communications in Heat and Mass Transfer*, Vol. 126, pp. 1-16, <https://doi.org/10.1016/j.icheatmasstransfer.2021.105479>
6. Bhattacharyya K., (2011): Dual Solutions in Unsteady Stagnation-Point Flow over a Shrinking Sheet, *Chinese Physics Letters*,vol. 28(8), pp.14, <http://dx.doi.org/10.1088/0256-307X/28/8/084702>.
7. Crane L.J. (1970): Flow past a stretching plate., *J. Appl. Math. Phys. (ZAMP)*, vol.21, pp.645-647.
8. Datta B.K., Roy P., Gupta A. S., (1985): Temperature field in the flow over a stretching sheet with uniform heat flux, *Int Commun Heat Mass Transfer*, vol.12, pp.89–94.
9. Dey D., Borah R.,(2021): Dual solutions of boundary layer flow with heat and mass transfers over an exponentially shrinking cylinder: stability analysis, *Latin American Applied Research*, Vol.50(4),pp.247-253, <https://doi.org/10.52292/j.laar.2020.535>
10. Ellahi R., Hayat T., Javed T., Asghar S., (2008): On the analytic solution of nonlinear flow problem involving Oldroyd 8-constant fluid, *Mathematical and Computer Modelling*, 48(8), pp. 1191-1200 DOI: 10.1016/j.mcm.2007.12.017.
11. Fadzilah A., Roslinda N., Norihan A., (2010): Numerical Solutions of Unsteady Boundary Layer Flow due to an Impulsively Stretching Surface, *journal of applied computer and science*, Vol.4(2), pp.25-30.
12. Hayat T, Abbas Z, Sajid M., (2006): Series solution for the upper convected Maxwell fluid over a porous stretching plate. *Phys Lett A*, vol.358, pp.396–403.
13. Hayat T, Sajid M. (2007): Analytic solution for axisymmetric flow and heat transfer of a 2nd-grade fluid past a stretching sheet. *Int J Heat Mass Transfer*, vol.50, pp.75–84.
14. Ishak A, Nazar R, Pop I. (2008): Uniform suction/blowing effect on flow and heat transfer due to a stretching cylinder. *Appl Math Modell*, vol.32, pp.2059–2066.
15. Ishak A, Nazar R.(2009): Laminar boundary layer flow along a stretching cylinder. *Eur J Sci Res*, vol.36(1), pp.22–29.
16. Jagan, K., Sivasankaran, S., (2022): Soret & Dufour and Triple Stratification Effect on MHD Flow with Velocity Slip towards a Stretching Cylinder. *Math. Comput. Appl.*, 27(25), pp.1-15 . <https://doi.org/10.3390/mca27020025>
17. Jauhri S, Mishra U., (2021): Dual Solutions of EMHD Nanofluid at Stretching Sheet with Mixed Convection Slip Boundary Condition, *Int. J. of Heat and Technology.*, 39(6), pp. 1887-1896.
18. Jauhri S, Mishra U., (2023): Numerical investigation of MHD nanofluid considering 2nd -order velocity slip effect over a stretching sheet in porous media, *Journal of Integrated Science and Technology.*, 11(2), pp. 478-485.
19. Jauhri S, Mishra U., (2022): A study of MHD fluid with 2nd-order slip and thermal flow over a nonlinear stretching sheet, *Int. J. of Applied Mechanics and Engineering.*, 27(2), pp. 98-114.
20. Lin H.T., Shih Y.P., (1980): Laminar boundary layer heat transfer along static and moving cylinders. *J Chin Inst Eng*, vol.3, pp.73–79.
21. Lin H.T., Shih Y.P., (1981): Buoyancy effects on the laminar boundary layer heat transfer along vertically moving cylinders. *J Chin Inst Eng*, vol.4, pp.47–51.
22. Mahapatra T, Gupta A. S., (2004): Stagnation-Point Flow of a Viscoelastic Fluid Towards a Stretching Surface, *International Journal of Non-Linear Mechanics* 39(5):811-820 DOI: 10.1016/S0020-7462(03)00044-1.
23. Mahapatra T.R.,Sidui S., (2016):“An analytical solution of MHD flow of two visco-elastic fluids over a sheet shrinking with quadratic velocity”, *Alexandria Engineering Journal*,vol.55(1), pp. 163-168, <https://doi.org/10.1016/j.aej.2015.12.01>.
24. Mishra U., Singh G., (2014): Dual solutions of mixed convection flow with momentum and thermal slip flow over a permeable shrinking cylinder, *Computers & fluids*, Vol.93, pp.107-115, <https://doi.org/10.1016/j.compfluid.2014.01.012>.
25. Mukhopadhyay S., (2013):MHD boundary layer slip flow along a stretching cylinder, *Ain Shams Engineering Journal*, Vol 4(2), Issue 2, Pp. 317-324, <https://doi.org/10.1016/j.aej.2012.07.003>.
26. Mukhopadhyay S., (2011): Chemically reactive solute transfer in a boundary layer slip flow along a stretching cylinder. *Front Chem Sci Eng*;5(3):385–91. <http://dx.doi.org/10.1007/s11705-011-1101-4>.
27. Nazar R., Ishak A., and Pop I., (2008): Unsteady Boundary Layer Flow over a Stretching Sheet in a Micropolar Fluid, *International Journal of Mathematical, Computational, Physical, Electrical and Computer Engineering*, Vol.2(2), pp. 108-112.
28. Vinita, Kumar Parveen, Poply Vikas, (2023): Mathematical Modelling of Magnetohydrodynamic Nanofluid Flow with Chemically Reactive Species and Outer Velocity Towards Stretching Cylinder, *Journal of Nanofluids*, vol. 12(4), pp.1067-1073.
29. Mahmood Z., Eldin S.M., Rafique K., Khan U.,(2023): Numerical analysis of MHD tri-hybrid nanofluid over a nonlinear stretching/shrinking sheet with heat generation/absorption and slip conditions, *Alexandria Engineering Journal*, Vol.76,pp. 799-819, <https://doi.org/10.1016/j.aej.2023.06.081>.
30. Wang CY. Flow due to a stretching boundary with partial slip – an exact solution of the Navier–Stokes equations. *Chem Eng Sci* 2002; 57: 3745–7.
31. Yasmeen T., Hayat T., Khan M., Imtiaz M., Alsaedi A., 2016: Ferrofluid flow by a stretched surface in the presence of magnetic dipole and homogeneous-heterogeneous reactions, *Journal of Molecular Liquids* 223., DOI: 10.1016/j.molliq.2016.09.028.
32. Zaimi K, Ishak A, Pop I, (2014): Unsteady flow due to a contracting cylinder in a nanofluid using Buongiorno's model, *Int J Heat Mass Transf*, vol.68, pp.509–513.
33. Z. Abbas, S. Rasool, M.M. Rashidi (2014): Heat transfer analysis due to an unsteady stretching/shrinking cylinder with partial slip condition and suction, *Ain Shams Engineering Journal*, vol. 6, pp. 939-945.